Health outcomes of 100% orange juice and orange flavored beverage: A comparative analysis of gut microbiota and metabolomics in rats

Kewen Wang [a,b], Yang Zhao [a], Lei Xu [a,b], Xiaojun Liao [a,**], Zhenzhen Xu [a,b,*]

[a] *College of Food Science and Nutritional Engineering, China Agricultural University, Beijing, 100083, China*
[b] *Institute of Quality Standard & Testing Technology for Agro-Products, Key Laboratory of Agro-food Safety and Quality, Ministry of Agriculture and Rural Affairs, Chinese Academy of Agricultural Sciences, Beijing, 100081, China*

ARTICLE INFO

ABSTRACT

A high intake of sugar-sweetened fruity beverage (FB) is associated with a higher risk of metabolic syndromes, but the health outcome of 100% fruit juice (FJ) intake remains unclear. We aim to reveal health outcomes of diet intervention (FJ or FB) with system profiling via interaction of gut microbiota and metabolomics in a rat (*Rattus norvegicus*) model. Firstly, the glucose, sucrose, fructose, and bioactive metabolites of FJ and FB were analyzed, and FJ possessed higher sucrose and flavonoids, while FB showed higher glucose and fructose. Secondly, C0 was set as the control group on Day 0, and a 4-week diet invention was performed to control, FJ-intake, and FB-intake groups with normal saline, FJ, and FB, respectively. The results showed that FJ improved alpha diversity and decreased the *Firmicutes/Bacteroidota* ratio (F/B ratio) of gut microbiota and prevented insulin resistance. However, FB possessed unchanged microbial diversity and enhanced F/B ratio, causing insulin resistance with renal triglyceride accumulation. In summary, FJ, although naturally containing similar amounts of total free sugars as FB, could be a healthier drink choice.

1. Introduction

In 2012, the United Nations announced that chronic non-communicable diseases (CNCD), such as cancer, diabetes, and heart disease, pose a considerable health burden than do infectious diseases. Tobacco, alcohol, and diet were targeted as the central risk factors in CNCD (Ng et al., 2009). Both tobacco and alcohol are regulated by governments to protect public health, leaving diet behind health crisis unchecked (Lustig et al., 2012). Globally, many governments have adopted diverse regulatory policies, including nutrition labeling, restrictions on food marketing, and taxation, to curb the epidemic of obesity and CNCD (Lartey et al., 2018; Vandevijvere et al., 2019).

Diet is foods and drinks regularly consumed, and its regulation is complicated. It is necessary to obtain a practical understanding of which foods and drinks contribute to health and well-being and which could be detrimental. As two commonest drinks, fruity beverages (FB) are defined as fruit-flavored drinks, calorie-containing carbonated drinks, vitamin water drinks, energy drinks, and sports drinks (Zheng et al., 2015), while fruit juice (FJ) is liquid obtained from the edible part of mature and fresh fruit or of fruit maintained in sound condition by suitable means

following CODEX STAN 247–2005 (CODEX STAN, 2005). Clear evidence shows that a high intake of FB is associated with a higher risk of metabolic syndromes, such as for overweight and obesity (Hagele et al., 2018), hypertension, type 2 diabetes, cardiovascular disease (Jayalath V H, Souza R J D, & V, 2015; Malik et al., 2010; Narain et al., 2016), as well as dental caries (Guido JA, Martinez Mier EA, & A, 2011) and even poor mental health (Freije et al., 2021). Unlike for FB, there is inconsistent evidence that drinking FJ poses a risk to human health, and there is conflict between the findings of observational studies, which can be influenced by confounders, and those of randomized controlled trials. Although no effect on weight gain was found in a meta-analysis of randomized controlled trials (D'Elia et al., 2021), longitudinal evaluation showed drinking 100% fruit juice was related to higher odds of becoming overweight (Shefferly et al., 2016). Moreover, a controlled clinical trial suggested that daily consumption of fruit juice had a positive effect on the intestinal microbiota and metabolic biomarkers of young women (Lima et al., 2019).

Recently, the interplay between host metabolism and associated gut microbiota has been a research hotspot (Laparra and Sanz, 2010; Monteiro et al., 2017). Notably, their joint characterization is conducive to

---

clarifying the effects of diet intervention on health outcomes (Posma et al., 2020). Certain plant foods that contain bioactive compounds may be more likely to drive microbial changes than others; however, complexity of food can make interpretation difficult (Willis and Slavin, 2020). Higher plant-based diet ratio was significantly associated with a higher relative abundance of *Bacteroides* and *Eubacterium*, amino acid biosynthesis pathways, and the pathway of pyruvate fermentation (Y. Li et al., 2021). In this work, a 4-week drink intervention study on rats was conducted to illuminate health outcomes for intake of FJ via interaction of gut microbiota and metabolomics compared with intake of FB.

2. Materials and methods

2.1. Drinks preparation

The orange flavor occupies the first position with 26.2% of the fruit juice market share (Neves et al., 2020). Hence, we chose 2 kinds of popular drinks from the local supermarket as the objects of our study. FB is a kind of orange-flavored beverage, or sugar-sweetened fruity beverage. It contains orange juice from concentrate and its label claims no less than 10% orange juice content. The ingredient list shows that FB contains water, high fructose corn syrup, granulated sugar, and food additives (citric acid, sodium citrate, and β-carotene), essence, and vitamin C. FJ is a kind of 100% orange juice not from concentrate, and its label claims 100% orange juice content without extra ingredient. All drink samples were sealed in their original packaging, stored at room temperature, and shaken before use. The rats only received one juice product per intervention group.

2.2. Measurement of 3 primary free sugar in drinks

The contents of glucose, fructose, and sucrose were determined according to the previous method with some modifications (B. Wang et al., 2021). The juice was diluted 5000 times and filtered using a 0.22-μm polytetrafluoroethylene membrane. Ion chromatography (ICS 3000+, Thermo Fisher Scientific, USA) system, consisted of (i) an ICS-3000 dual pump, (ii) an automated sample injector (Dionex AS autosampler), (iii) working electrode: Gold (Au), reference electrode: pH electrode (Dionex, Germany), (iv) PA20 anion analysis column (3 mm × 150 mm), (vi) PA20 guard column (4×50 mm), was used. Mobile phase A was water and B was 200 mM NaOH. The elution procedure was 0–20.00 min, 5% B; 20.00–20.01 min, 5%–20% B; 20.01–30.00 min, 20% B; 30.00–30.01 min, 20%–100% B; 30.01–40.00 min, 100% B; 40.00–40.01 min, 100%–5% B; 40.01–50.00 min, 5% B. The injection volume, flow rate, and column temperature were 10 μL, 0.400 mL/min, and 30 °C, respectively.

2.3. Animal experiment

All animal experiments were performed in the lab of the Institutional Animal Care and Use Committee of Beijing Vital River Laboratory Animal Technology Co., Ltd. All experimental procedures described here were conducted following the National Institutes of Health Guidelines on the Care and Use of Laboratory Animal of Institutional Animal Care and Use Committee of Beijing Vital River Laboratory Animal Technology Co., Ltd. The approve code is SCXK-2016–0006. The permission code is P2021032.

Six-to eight-week-old SD (*Rattus norvegicus*) rats (male; SPF; the mean weight of 209 g) were purchased from Vital River Laboratory Animal Technology Co. Ltd (Beijing, China). The animal feeds were purchased from Keao Xieli Feed Co., Ltd (Beijing, China), and the primary nutrients of animal feed are shown in Table S1. The rats were kept under controlled light conditions (12 h light-dark cycle) with free access to feed and water throughout the entire intervention.

The design of drink intervention study is shown in Fig. 1. The rats were acclimatized for 7 days, and the weight, fasting blood glucose (FBG), total cholesterols (TC), total triglycerides (TG), high-density
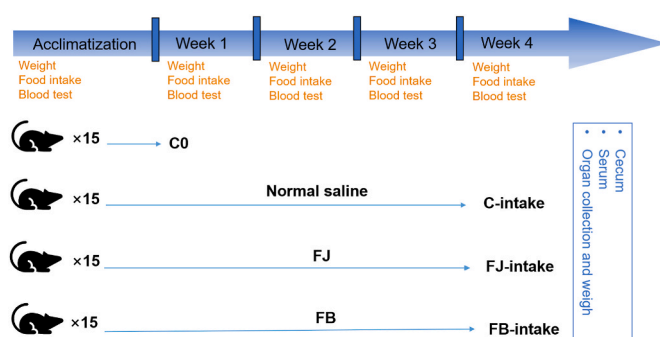

Fig. 1. The specific experiment design of the animal experiment.

lipoprotein cholesterol (HDL-C), and low-density lipoprotein cholesterol (LDL-C) were recorded on the last day of acclimatization. When the rats were adapted to the experiment condition during the first week, body weight, FBG, TC, TG, HDL-C, and LDL-C were measured to divide these rats into 4 groups, denoted as C0, control, FJ-intake, and FB-intake, respectively. After grouping, there are no significant differences in these indices among groups (Fig. S1).

For C0, cecum, and serum samples were directly collected after 7 days of acclimatization and stored at −80 °C until analysis. Then, rats were dissected to obtain kidney, brain, liver, fat from subcutaneous and epididymis, colon, intestine, and cecum. The organ mass was recorded and the organs were stored at −80 °C until analysis.

The control and 2 intervention groups (control, FJ-intake, and FB-intake) proceeded with formal intervention for 28 days. Under the regular diet, the rats were gavaged with normal saline, FJ, and FB for control, FJ-intake, and FB-intake, respectively (twice per day) at the same time every day. Each rat was given the equivalent of one adult (60 kg) drinking 300 mL of drinks a day. According to previous study, the dose conversion between rat and human is 6.2 (Nair and Jacob, 2016). If an adult (60 kg) consumes 300 mL of orange juice daily, the equivalent dose for rats is 31 mL/kg (300 mL/60 kg*6.2 = 31 mL/kg). Hence, the specific volume of gavage was calculated as 31 times the volume of each rat's last measured body weight (for example, if the last measured weight of a rat is 0.2 kg, its gavage volume is 6.2 mL per day). During the 28-day diet, the weight, FBG, TC, TG, HDL-C, and LDL-C were recorded once per week. On the last day, samples from the 3 groups were collected and stored under the same condition as C0. The organ index was calculated based on the ratio of organ mass to body weight.

2.4. Gut microbiota analysis

Eight rats were randomly selected from each group for 16S rRNA sequencing. The corresponding cecum sample from the chosen rat was snap-frozen with liquid nitrogen following collection and was stored in a −80 °C refrigerator. Then, 32 cecum samples were transported to Majorbio Bio-pharm Technology Co., Ltd (Shanghai, China) on dry ice.

The genomic DNA of cecum samples was extracted using the DNA Extract Kit (Omega Bio-Tek, USA). The DNA was checked on 1% agarose gel, and the concentration and purity of DNA were determined using NanoDrop 2000 UV–vis spectrophotometer (Thermo Scientific, USA). The 16S rRNA genes of V3–V4 regions were amplified with specific primers (338F and 806R) using ABI GeneAmp® 9700 PCR thermocycler (ABI, USA). After initial denaturation at 95 °C for 3 min, 30 cycles of amplification were performed as follows: 95 °C for 30 s, 55 °C for 30 s, and 72 °C for 45 s followed by a single extension at 72 °C for 10 min to amplify the 16S rRNA gene. The PCR product was verified on a 2% agarose gel and purified using the AxyPrep DNA Gel Extraction Kit (Axygen Biosciences, USA) and quantified using Quantus™ Fluorometer (Promega, USA). Purified amplicons were pooled into equimolar and paired-end sequenced on an Illumina MiSeq PE300 platform (Illumina, USA). The raw 16S rRNA gene sequencing reads were demultiplexed,

quality-filtered by fastp version 0.20.0, and merged by FLASH version 1.2.7. Operational taxonomic units (OTUs) with a 97% similarity cutoff were clustered using UPARSE version 7.1, and chimeric sequences were identified and removed. The taxonomy of each OTU representative sequence was analyzed by RDP Classifier version 2.2 against the Silva v138 16S rRNA database using a confidence threshold of 0.7.

2.5. Metabolite analysis

The metabolite analysis was performed by ultrahigh-pressure liquid chromatography coupled with a quadrupole time-of-flight mass (UHPLC-QTOF MS). The samples were subjected to a reversed-phase chromatography using an LC system (SCIEX, USA). Mass spectrometric analysis was performed with a QTOF MS with a DuoSpray ion source (TripleTOF 6600, SCIEX, USA). Quality control (QC) samples were made by pooling equal aliquots of each sample together in an analytical run (Johnson et al., 2018). The QC sample was injected and analyzed at regular intervals of every 6 samples in UHPLC-QTOF MS acquisition. These QC sample data were used to monitor the reproducibility and stability of the analytes in samples during the analysis (Theodoridis et al., 2012).

2.5.1. Drinks

The metabolomics was conducted on 2 drinks according to the previous method with modifications (K. Wang and Xu, 2022). The 2 drinks were filtered using a 0.22-μm polytetrafluoroethylene membrane and 2 drinks with 6 replicates each were obtained. The separation column is ACQUITY UPLC HSS T3 (1.8 μm, 2.1×100 mm, Waters, USA), maintained at 40 °C, and the autosampler was maintained at 4 °C. The injection volume and flow rate were 2 μL and 0.300 mL/min. Mobile phases A and B were 0.2% formic acid in water and acetonitrile, respectively. Solvent gradient was as follow: 0–11.50 min, 5%–30% B; 11.50–11.51 min, 30–100% B; 11.51–15.00 min, 100% B; 15.00–15.01 min, 100%–5% B; 15.01–18.00 min, 5% B. The SWATH with a cycle time of 545 ms was composed of a TOF MS scan (accumulation time, 50 ms; CE, 10 eV) and a series of product ion scans (accumulation time, 30 ms each; CE, 35 eV, CES 15 eV) of 15 Q1 windows of 60 Da from m/z 100–1000.

2.5.2. Kidney lipidomic samples

The lipidomics was conducted on kidney samples according to previous methods with modifications (Z. Chen et al., 2020; Tu et al., 2017; K. Wang et al., 2021). Thirty-mg frozen kidney tissue was weighed and homogenized in 600-μL extract (MTBE: MeOH = 5:1, v/v) using the homogenizer, and 1-μL internal standard of Cer-d7 (100 μg/mL) was added. The solution was vortexed for 30 s, followed by 10 min of sonication, and centrifugation at 3000 rpm for 15 min. The upper organic layer was collected. An additional 600-μL MTBE was added to the bottom layer for re-extraction. The re-extraction was repeated twice. The pooled organic layer was evaporated using a termovap sample concentrator. Before subsequent analysis, the dry extract was reconstituted using 100-μL DCM: MeOH (1:1, v/v). The separation column is Phenomenex Kinetex C18 column (1.7 μm, 2.1×100 mm, Waters, USA), maintained at 55 °C, and the autosampler was maintained at 4 °C. The injection volume was 2 μL and 6 μL in positive and negative modes, respectively. The mobile phase consisted of A: 5 mM $H_3CCOONH_4$+40% $H2O$+60% CAN, B: 5 mM H_3COONH_4+10% ACN+90% IPA was carried with elution gradient as follows: 0 min, 40% B; 12 min,100% B; 13.5 min, 100% B; 13.7 min, 40% B; 18 min, 40% B, which was delivered at 0.3 mL/min. The Triple TOF mass spectrometer was used for its ability to acquire MS/MS spectra on an IDA mode. The acquisition software (Analyst TF 1.7, AB SCIEX) continuously evaluates the full scan survey MS data in this mode. It collects and triggers the acquisition of MS/MS spectra depending on preselected criteria. In each cycle, 11 precursor ions whose intensity greater than 100 were chosen for fragmentation at collision energy (CE) of 35 V (15 MS/MS events with product ion

accumulation time of 50 ms each). ESI source conditions were set as follows: Ion source gas 1 as 60, Ion source gas 2 as 60, Curtain gas as 30, source temperature 550 °C, Ion Spray Voltage Floating (ISVF) 5500 V or − 4500 V in positive or negative modes, respectively.

2.5.3. Cecum content samples

The cecum content samples were performed according to previous methods with modifications (Tian et al., 2012; Xie et al., 2013). And 300-mg of cecum contents was weighed with 1.5-mL methanol-water (v: v = 1:1, 4 °C) solution added. The mixture was vibrated for 30 s, frozen in liquid nitrogen for 30 s, then thawed in water at room temperature, and repeated 3 times. After the last thawing, an ultrasound was performed for 30 s followed by 10-s vibration and 30-s standing; then, the process was repeated 5 times. Centrifugation was performed at 15000 g for 5 min at 4 °C. Finally, the supernatant was filtered using a 0.22-μm nylon membrane for analysis. The separation column is C18 (1.7 μm, 2.1×100 mm, Waters, USA), maintained at 40 °C, and the autosampler was maintained at 4 °C. The injection volume and flow rate were 2 μL and 0.300 mL/min. Mobile phases A and B were 0.1% formic acid in water, and 0.1% formic acid in acetonitrile, respectively. For cecum samples, solvent gradient was as follow: 0–0.10 min, 5% B; 0.10–2.00 min, 5–13% B; 2.00–4.00 min, 13–28% B; 4.00–8.50 min, 28–40% B; 11.50–13.00 min, 40–70% A; 13.00–13.50 min, 73–100% B; 13.50–16.00 min, 100% B; 16.00–20 min, 5% B. The SWATH with a cycle time of 550 ms was composed of a TOF MS scan (accumulation time, 50 ms; CE, 10 eV) and a series of product ion scans (accumulation time, 30 ms each; CE, 35 eV, CES 15 eV) of 15 Q1 windows from m/z 50–1200.

2.5.4. Serum content samples

The serum content samples were performed according to a previous method with modifications (Lin et al., 2011). The serum was thawed in a refrigerator at 4 °C. After thawing, the serum was rotated for 5 s. The 400-μL methanol was added to 200-μL serum, and the mixture was rotated for 10 s and stood at room temperature for 15 min. Then, centrifugation was performed at 10000 g for 20 min at 4 °C. Finally, the supernatant was filtered using a 0.22-μm nylon membrane for analysis. Totally, 120 samples of the cecum and serum samples (60 samples each) from all the rats were obtained. The separation column is C18 (1.7 μm, 2.1×100 mm, Waters, USA), maintained at 40 °C, and the autosampler was maintained at 4 °C. The injection volume and flow rate were 2 μL and 0.300 mL/min. Mobile phases A and B were 0.1% formic acid in water, and 0.1% formic acid in acetonitrile, respectively. For serum samples, solvent gradient was as follow: 0–0.10 min, 5% B; 0.10–1.50 min, 5–13% B; 1.50–2.50 min, 13–28% B; 2.50–5.50 min, 28–40% B; 5.50–7.50 min, 40–70% A; 7.50–15.00 min, 70–90% B; 15.00–16.00 min, 90–100% B; 16.00–19.00 min, 100% B; 19.01–22.00 min, 5%B. The SWATH with a cycle time of 550 ms was composed of a TOF MS scan (accumulation time, 50 ms; CE, 10 eV) and a series of product ion scans (accumulation time, 30 ms each; CE, 35 eV, CES 15 eV) of 15 Q1 windows from m/z 50–1200.

2.6. Data processing and statistical analysis

Mean values with relative standard deviation (RSD) were calculated, and statistical analyses were performed using R 4.0.3 (Inc., MA, USA). To compare glucose, sucrose, fructose contents, and the fructose-to-glucose ratio in 2 drinks, the student's t-test was conducted. For comparing food intake, FBG, TC, TG, HDL-C, LDL-C, body weight change, and organ mass index in rats from different groups, ANOVA followed by the Bonferroni test was conducted.

For gut microbiota analysis, the alpha diversity (ACE, Chao, and Sobs estimator) and beta diversity of PCoA based on weighted UniFrac distances were analyzed using R 4.0.3. To compare alpha diversity, the Kruskal-Wallis rank-sum test followed by Game-Howell was conducted. Linear discriminant analysis effect size (LEfSe) was used to identify the

microbial taxa that significantly differed between FJ-intake and FB-intake groups, with a threshold of linear discriminant analysis (LDA) score >2.0. Functional pathway analysis of gut microbiota was performed using the PICRUSt2 approach, based on the Kyoto Encyclopedia of Genes and Genomes (KEGG) database with the 16S rRNA gene sequencing data (Majorbio Cloud Platform). Differences in pathways between FJ-intake and FB-intake groups were identified using LEfSe with a threshold LDA score of >2.0.

For metabolite analysis, UHPLC-QTOF MS data were processed by MS-DIAL 4.60 to get the MS1 raw peak list and intensity. The parameters were set as follows: MS1 and MS2 tolerance were 0.01 Da and 0.025 Da in peak extraction, and the maximum charge number was 2. MS1 and MS2 tolerance were 0.01 Da and 0.05 Da in qualitative extraction, and the retention time deviation in peak alignment was 0.2 min. The MS1 deviation was 0.015 Da, the detection rate reached 80% in at least one group, and the S/N ratio (maximum in the sample/mean in the blank sample) was 5. The exported MS1 peak list was analyzed by Microsoft Office Excel 2020 (Microsoft Corporation, USA) to remove the MS1 features with a detection rate was <80% or RSD >30% in the QC group (Lachowicz and Oszmianski, 2018). For kidney lipidomics samples, the MS1 features with p-value <0.05 and FC > 1.2 were selected as characteristic markers for further identification with a built-in lipid database in MS-DIAL (K. Wang et al., 2022). For drinks, the MS1 features with p-value <0.05, FC > 5, and variable importance for projection (VIP) > 1.5 based on the orthogonal partial-least squares discriminant analysis (OPLS-DA) model were selected as characteristic markers for further identification. For cecum and serum samples, all the MS1 features were further identified. Specifically, the MS1 features that met the above conditions were identified by exporting their MS2 spectra from MS-DIAL 4.60 into MS-FINDER 3.50 for putative annotation by matching the databases, such as MassBank of North America, RIKEN PlaSMA, ReSpect, HMDB, lipid maps, PubChem, and FooDB. The parameters, MS1 tolerance, and MS2 tolerance were set as 10 ppm and 15 ppm, respectively.

For correlation analysis, spearman correlations were conducted on GraphPad Prism 8 (GraphPad Software, USA). The correlation with coefficient >0.5 and p-value <0.05 was considered a significant correlation and then plotted by Microsoft Office Excel 2020 or Cytoscape (v3.4.0).

3. Results

3.1. Fruity beverage increased food intake and body weight change

Based on the product's labels (Table S2), the energy of FJ (205 kJ/100 mL) is slightly higher than that of FB (183 kJ/100 mL), and the carbohydrate contents in FJ and FB are similar, which are 100 g and 94 g per liter, respectively. Moreover, FJ contains 13.25 g glucose, 15.19 g fructose, and 30.66 g sucrose per liter, while FB contains 19.37 g glucose, 28.14 g fructose, and 17.31 g sucrose per liter (Fig. 2A). Glucose and fructose contents in FB are higher than those in FJ, while sucrose content in FJ is significantly higher than that in FB. The increased glucose and fructose contents in FB should come from the added high fructose corn syrup, which was also claimed on the labels. Then, the fructose-to-glucose ratio in FJ is significantly lower than that in FB, which are 1.1 and 1.5, respectively (Fig. 2B).

During the formal intervention, no matter what types of drinks they ingested, it would not affect the rats' FBG and blood routine examination indices (Fig. S2 A~E). The food intake of all the 3 groups increased as the rats grew older; specifically, during the first two weeks, the food intake of FB-intake group was significantly lower compared to control and FJ-intake groups (Fig. 2C). However, during the third and fourth weeks, the opposite phenomenon appeared: food intake in FB-intake and control groups was significantly higher than in FJ-intake groups (Fig. 2C). The weight change is generally consistent with the food intake changes (Fig. 2D). It is worth noting that FJ with higher labeled energy led to a lower weight gain than FB.

3.2. Fruity beverage induced renal disorder

Remarkably, a significant increase of kidney mass index is found in FB-intake group compared with control and FJ-intake groups (Fig. 2E). In contrast, no significant difference in the other organ indices is found (Figs. S2–F). The increase of kidney mass was statistically associated with the whole injury process of renal disorders (Craig et al., 2015; H. Liu et al., 2017). Lipids are attributed to ~3% of human renal wet weight. Regardless of whether the injury is acute or chronic, either intrarenal or circulatory lipid disturbances are exhibited in various renal disorders (Su et al., 2017). Hence, we highly speculated that the intrarenal lipids were altered and lipidomics analysis of kidney was further
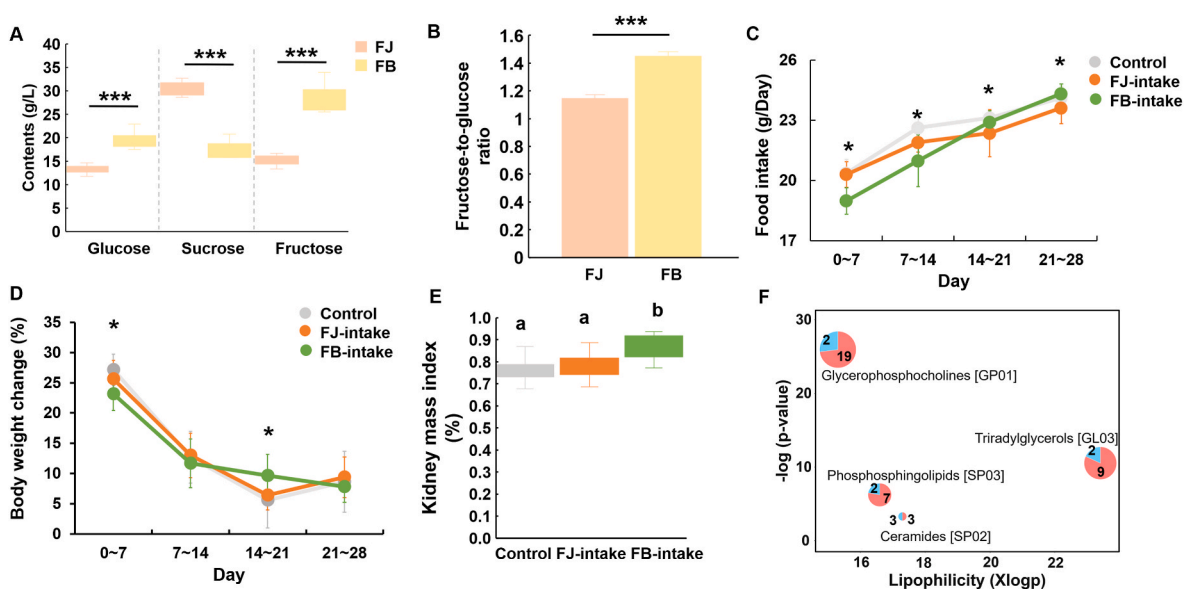

Fig. 2. A The contents of glucose, sucrose, and fructose in FJ and FB. B The fructose-to-glucose ratio in FJ and FB. C Food intake, D body weight change, and E kidney mass index of rats during acclimatization and formal intervention. F ChemRICH impact plot of chemical similarity enrichment analysis in the abnormal group (FB-intake group) compared to the normal group (combined control and FJ-intake groups).

conducted to verify the renal disorder in FB-intake group (Fig. S3 and Table S3). According to the above results, control and FJ-intake were combined into the normal group to compare with the abnormal group of FB-intake. The ChemRICH plot illustrates significantly altered lipid classes. Most lipids in triradylglycerols [GL03], glycerophosphocholines [GP01], and phosphosphingolipids [SP03] are significantly higher in FB-intake group, while half lipids in ceramides [SP02] are elevated in FB-intake group (Fig. 2F). The altered lipids in the kidney further proved potential chronic renal disorder in FB-intake group.

For A and B, the student's t-test was conducted.

For C, D, and E the ANOVA followed by the Bonferroni test was conducted.

For F, the size of the cluster indicates the number of metabolites within the class. Red in a cluster is the percentage of rising lipids in the class, and blue in a cluster is the percentage of decreasing lipids in the class. The number shows the quantities of rising and decreasing lipids. The X-axis shows the median of Xlogp, which correlates with the lipophilicity of classes, so polar classes are shown on the right side of the

plot. The y-axis shows the negative log of p-value, so significantly important classes are shown at the top of the plot.

Different letters of the same index represent significant differences (p-value <0.05).

*, p-value < 0.05; ***, p-value < 0.001.

3.3. Fruit juice increased the richness of gut microbiota and decreased Firmicutes/Bacteroidota ratio

A total of 2,361,607 sequences are obtained from 32 cecum content samples, and sequencing quality is assessed using the rarefaction curve and rank abundance curve (Fig. S4). PCoA analysis based on ANOSIM demonstrates differences between the 4 groups (p-value = 0.012, Fig. 3A). In particular, C0 on the left of PCoA was separated from the other three groups, indicating the gut microbiota changes of rats were age-dependent. Compared to control, FJ-intake group possesses higher alpha diversity as measured by Ace, Chao, and Sobs indices, while FB-intake group shows similar alpha diversity (Fig. 3B). Drinking FJ tends
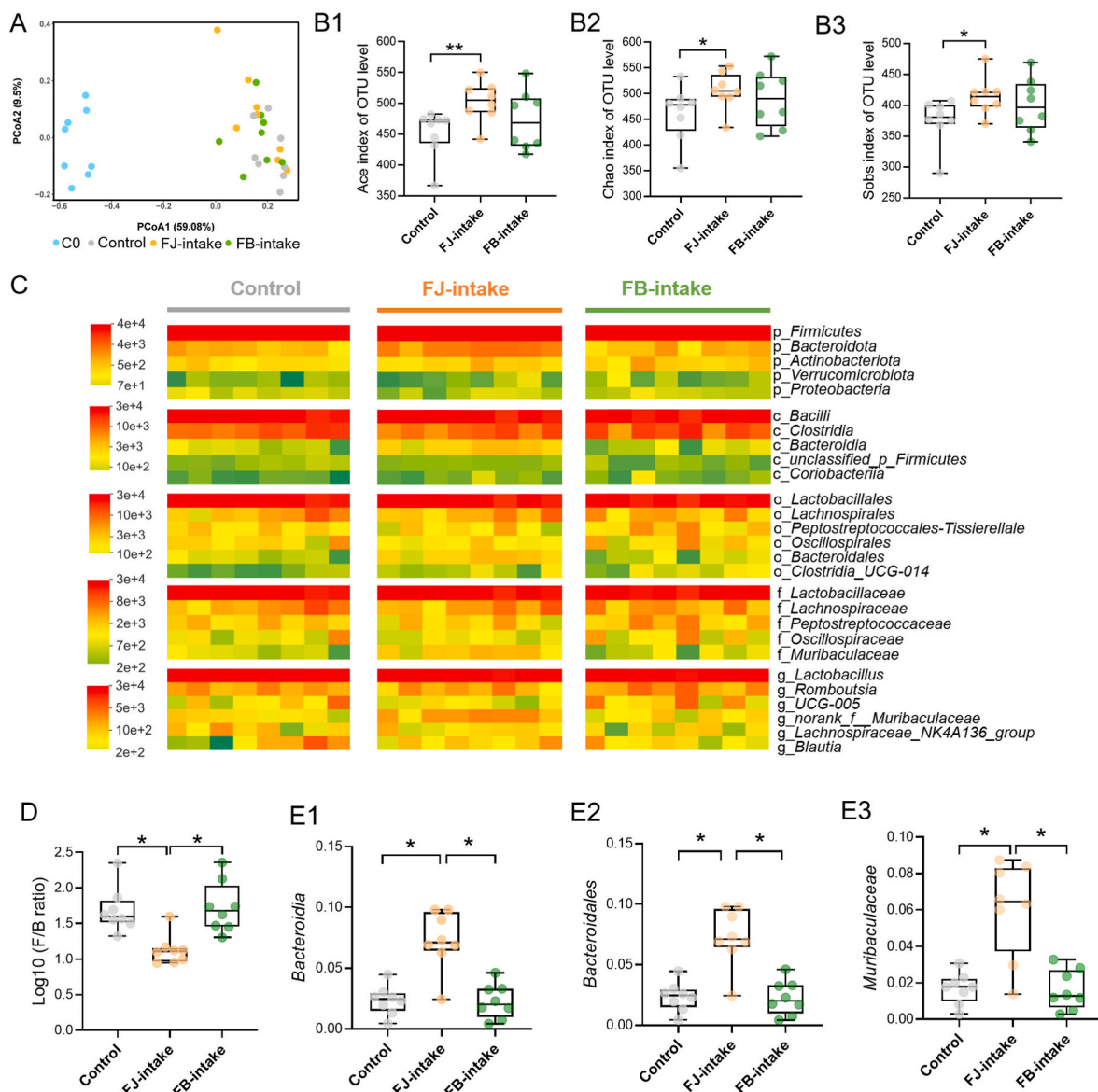

Fig. 3. A PCoA plot of beta diversity at OTU level with Weighted UniFrac distances followed by ANOSIM test. B Bar plots of the alpha diversity of B1 Ace, B2 Chao, and B3 Sobs at the OTU level. C An overview of the most abundant phyla, class, order, family, and genus in control, FJ-intake, and FB-intake groups; the taxa levels were determined by summing the OTUs and are presented by relative abundance. D Boxplot of *Firmicutes/Bacteroidota* ratio (F/B ratio), and E relative abundance of *Bacteroidia*, *Bacteroidales*, and *Muribaculaceae*.

to increase alpha diversity over drinking FB, although not significantly.

A broad overview of microbial taxonomic data is displayed in Fig. 3C, showing the abundance variance of high-abundance microorganisms in different groups. Firmicutes, Bacteroidetes, Actinobacteria, Verrucomicrobiota, and Proteobacteria are the top five phyla. Notably, Firmicutes and Bacteroidota are the dominant phyla in each sample and their total relative abundance reached 98.27 ± 1.10% (C0), 98.68 ± 0.54% (control), 98.35 ± 0.77% (FJ-intake), and 97.99 ± 1.19% (FB-intake). Moreover, a significantly reduced F/B ratio is revealed in FJ-intake group against control and FB-intake groups (Fig. 3D). The reduced F/B ratio in FJ-intake group mainly results from the increase of Bacteroidota (phylum). Especially, Bacteroidia (class), Bacteroidales (order), and Muribaculaceae (family) all come from the same clado-genesis of Bacteroidota (phylum), and they increase significantly in FJ-intake group against both control and FB-intake groups (Fig. 3E).

For B, D, and E, the Kruskal-Wallis rank-sum test followed by Game-Howell was conducted.

*, p-value < 0.05; **, p-value < 0.01; ***, p-value < 0.001.

3.4. Flavonoids in fruit juice are negatively correlated with Firmicutes/Bacteroidota ratio

To find the constant differential bioactive metabolites, metabolomics was conducted on FJ and FB. Totally, 159 potential markers are determined via OPLS-DA model and S-plot (Fig. S5). The potential markers with fold change (FC) value > 5 are identified, and they are mainly amino acids, sugars, organic acids, and flavonoids (Table S4). Interestingly, 8 flavonoids, which are naringenin, quercetin, hesperetin, nobiletin, narirutin, vicenin 2, didymin, and hesperidin are significantly higher in FJ, and their FC values between FJ and FB are 11.3 on average, with quercetin and hesperetin achieving the higher FC value of 28.3 and 26.2 (Fig. 4 and Table S4).

These findings guided multiple correlation analysis between the 8 flavonoids and markedly altered gut microbiota. The markedly altered gut microbiota is obtained with LDA scores >2 through LEfSe analysis (Fig. 5A). Fifteen bacterial taxa from Bacteroidetes and Desulfobacterota significantly increased in the FJ-intake group, while the other 15 bacterial taxa from Firmicutes and Actinobacteriota markedly increased in the FB-intake group. The correlation analysis illustrates that nobiletin and hesperetin possess the highest number of significant correlations, while vicenin 2 shows the lowest number of significant correlations (Fig. 5B). In terms of microbiota, bacterial taxa from Bacteroidetes and Firmicutes exhibit the highest number of significant positive and negative correlations with flavonoids, respectively. Similar to bacterial taxa from Bacteroidetes, bacterial taxa from Desulfobacterota are positively correlated with flavonoids as well, while bacterial taxa from

Actinobacteriota are the opposite (Fig. 5C).

Additionally, it is evident that except for vicenin 2, the other 7 flavonoids show significant negative correlations with the F/B ratio (Fig. 5B). The aforementioned results confirmed that higher flavonoids in FJ were conducive to improving bacterial taxa from Bacteroidetes and Desulfobacterota, while they were detrimental to the growth of bacterial taxa from Firmicutes and Actinobacteriota, hence achieving a decreased F/B ratio.

For B, node size is proportional to the number of significant correlations. Nodes are colored according to groups: orange—juice flavonoids and green—gut microbiota. Solid edges—positive correlations, marquee equal dash edges—negative correlations. Only correlations with correlation coefficient >0.5 and p-value <0.05 are displayed in network graphs.

For C, bacterial taxa with an LDA score >2.0 are written in black, while the others are written in white.

3.5. Distinct impacts of fruit juice and fruity beverage on microbial function and corresponding metabolites

To explore the role of gut microbiota in rat response to 2 drinks, a total of 309 functional KEGG categories were obtained by PICRUSt2. Among them, 17 KEGG categories (level 3) significantly differ between FJ-intake and FB-intake groups (Fig. 6A). FJ-intake group, which was characterized by bacterial taxa from Bacteroidetes and Desulfobacterota, stimulated the functional pathways of sphingolipid metabolism, alpha-linolenic acid metabolism, and glycosphingolipid biosynthesis, while FB-intake group, which was characterized by bacterial taxa from Firmicutes and Actinobacteriota, stimulated the functional pathways of insulin resistance. Also, about half of the 17 categories were related to metabolism (KEGG level 1), indicating drinks could primarily alter microbial metabolism.

Cecum and serum metabolites are sensitive to drinks and are tightly involved in functional pathways. C17-sphinganine, belonging to sphingolipid, was identified in the serum of rats, and it was higher in FB-intake group compared to FJ-intake group, with an FC value of 2.3. Further, it negatively correlates with sphingolipid metabolism (Fig. 6B). C17-sphinganine in serum is a specific biomarker of renal disorder (Lin et al., 2012), and its enhanced level in FB-intake group might indicate a potential chronic renal disorder. Dimethyl-L-arginine (ADMA) is recognized as an essential biomarker of metabolic syndrome (Etxeberria et al., 2015; Sibal et al., 2010), which is positively correlated with many insulin-resistant states and thus interferes with insulin signaling (Sydow et al., 2005), increasing the risk of diabetes, hypertension, and hypercholesterolemia (De Gennaro Colonna, Bianchi, Pascale, Ferrario, Morelli, Pascale, et al., 2009; Siervo et al., 2011). Also, ADMA is generated
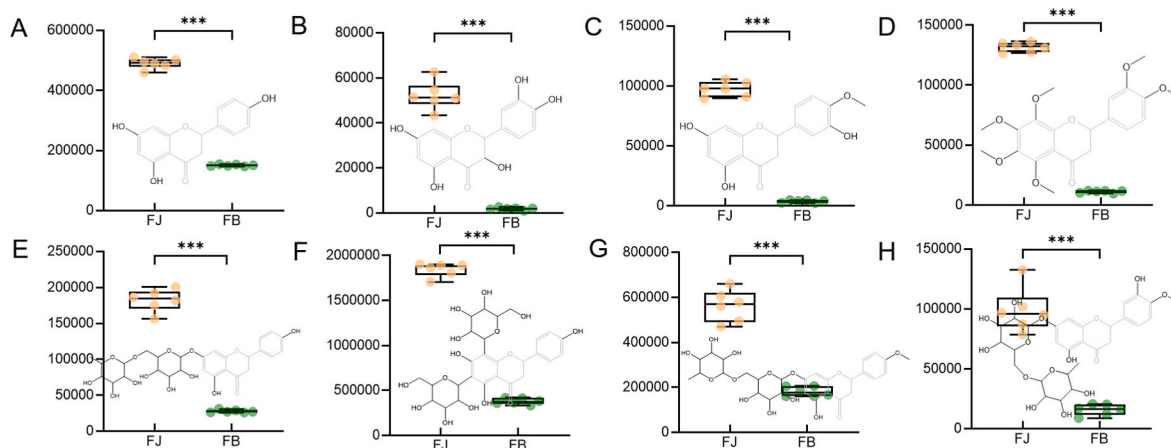

Fig. 4. The relative contents of 8 identified flavonoids in FJ and FB: A naringenin, B quercetin, C hesperetin, D nobiletin, E narirutin, F vicenin 2, G didymin, and H hesperidin.
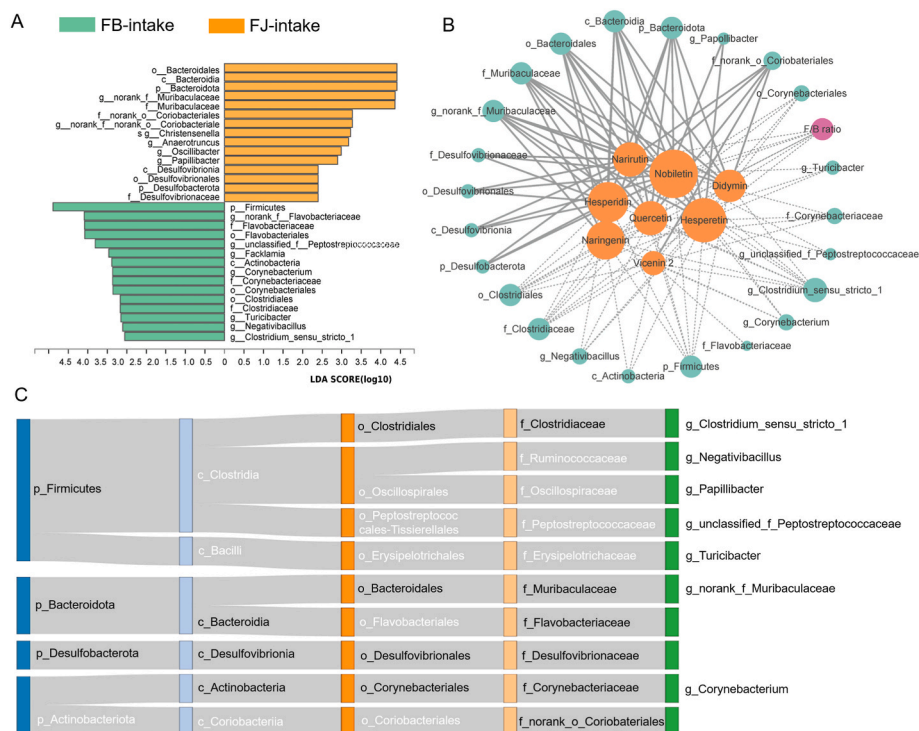
Fig. 5. A LEfSe bar of gut microbiota (from phylum to the genus level) with LDA score >2.0 between FJ-intake and FB-intake groups. B Spearman correlations between juice flavonoids and gut microbiota. C Taxonomic diagram of bacterial taxa in the LEfSe bar using Sankey plots.

by catalyzing the transfer of methyl groups from S-adenosyl-L-methionine (SAM) to arginine in target proteins (Hong et al., 2012). In this work, ADMA and SAM in cecum show significantly positive and negative correlations with insulin resistance (Fig. 6C and D), displaying the transfer of SAM into ADMA and hence causing insulin resistance. Additionally, the excess fructose in FB may partly be contributed to renal disorder via fast lipid accumulation (Fig. 6E), which is detailed in the discussion.

KHK, ketohexokinase; HK, hexokinase; ALDOB, aldolase B; DHAP, dihydroxyacetone phosphate; F1P, fructose-1-phosphate; GA, glyceraldehyde; SM, sphingomyelin; Cer, ceramide; FA, fatty acid; TAG, triacylglycerol; DAG, diacylglycerol; MAG, monoacylglycerols; PC, choline glycerophospholipid; PE, phosphatidylethanolamine; LPC, lysophosphatidylcholine; LPE, lysophosphatidylethanolamine; SAM, S-adenosyl-L-methionine; CDP-choline, cytidine diphosphate-choline.

4. Discussion

The NOVA food classification divides foods into four categories based on food processing degrees. It divides foods into four categories: unprocessed and minimally processed foods, processed culinary ingredients, processed foods, and ultra-processed foods (Monteiro et al., 2017). FB and FJ belong to ultra-processed food and minimally processed food, respectively. Although FAO guidelines appeal to promote the consumption of minimally processed foods and avoid the use of ultra-processed foods, the consequence of food processing degrees on health outcomes was not adequately illustrated (Food and Agriculture Organization of the United Nations, 2015).

Metabolic syndrome, an essential part of the epidemiology of CNCD, would raise the risk of individuals developing obesity, diabetes mellitus, insulin resistance, and atherosclerotic cardiovascular disease (Kotlyarov and Bulgakov, 2021; Markopoulou et al., 2019; Neergaard et al., 2017; Vega, 2004). It mainly results from a long-term diet imbalance and microbial dysbiosis, affecting collaborative metabolic pathways (Remely and Haslberger, 2017). Insulin resistance is one of the most

accepted unifying theories explaining the pathophysiology of metabolic syndrome (Mikhail, 2009). We found that the microbial function indicated an enhanced insulin resistance pathway, which has been identified as a potential contributor to metabolic syndrome in the host (Caricilli and Saad, 2013; He and Li, 2020). Moreover, insulin resistance plays an essential role in renal disorder (De Cosmo, Menzaghi, Prudente and Trischitta, 2013). In other words, renal triacylglycerol accumulation, as a marker of lipotoxicity, is associated with insulin resistance (Guebre-Egziabher et al., 2013; Unger and Scherer, 2010). We speculated that the upregulated insulin resistance pathway led to renal triacylglycerol accumulation and increased kidney mass index, which could cause potential chronic renal disorder in FB-intake group. Additionally, insulin plays a dominant role in regulating food intake (Rezek, 1976), and individuals who present with insulin resistance have a higher preference for food, likely due to a reduction in the ability of insulin to inhibit satiety (Tiedemann et al., 2017).

Glucose and fructose can suppress energy intake, but this effect is mainly in the short term. In young men, either 75 g (G. Harvey et al., 2002) or 50 g (Rogers et al., 1988) of glucose in drinks reduced food intake 1 h later. Consumption of 50 g fructose in a drink suppresses energy intake to an even greater extent at test meals from 38 min to 2.25 h later (Anderson, 1995; Anderson and Woodend, 2003; A. G. Harvey, Catherine Nicole, Woodend, & Wolever Thomas, 2002). Consistent with our results, FB containing significant higher glucose and fructose contents effectively reduced the food intakes of rats in the early stage, but after 2 weeks, the food intakes of rats in FB-intake group increased significantly, which was higher than that in control and FJ-intake groups in the long term. Combined with the enhanced insulin resistance pathway, FB-intake group might gradually develop insulin resistance after the 2-week intervention, resulting in increased food intake and weight gain.

Moreover, the excess fructose in FB may partly be contributed to renal disorder via fast lipid accumulation (Fig. 6E). Fructolysis bypasses glycogen synthase, and the enzymolysis rate of fructose kinase (ketohexokinase, KHK) is much higher than glucose kinase (hexokinase, HK)
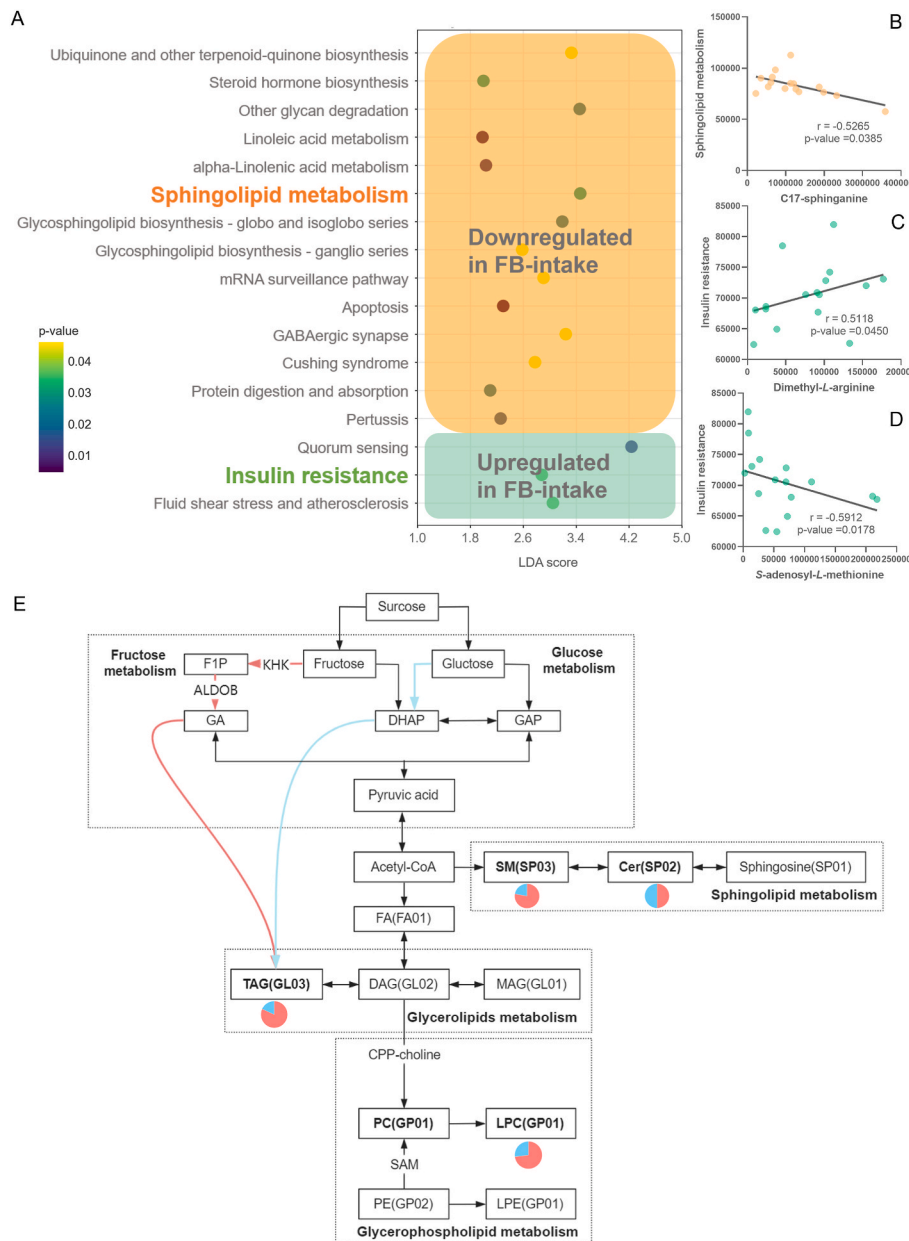
Fig. 6. A The bubble plot shows significantly varied KEGG categories of PICRUSt2 findings between FJ-intake and FB-intake groups. B Spearman correlations between C17-sphinganine in serum and functional pathway of sphingolipid metabolism. C Spearman correlations between dimethyl-L-arginine in the cecum and functional pathway of insulin resistance. D Spearman correlations between S-adenosyl-L-methionine in the cecum and functional pathway of insulin resistance. E Pathways are associated with glucose and lipid metabolism. The arrow next to the lipid represents changes in FB-intake group compared to FJ-intake group. Red in a cluster is the percentage of rising lipids in the corresponding class, and blue in a cluster is the percentage of decreasing lipids in the corresponding class. (For interpretation of the references to color in this figure legend, the reader is referred to the Web version of this article.)

(Asipu, Hayward, O'Reilly and Bonthron, 2003). Aldolase B (ALDOB) directly splits fructose-1-phosphate into dihydroxyacetone phosphate (DHAP) and glyceraldehyde (GA) without overcoming the rate-limiting phosphofructokinase (PFK) (Bulik et al., 2016). Hence, fructose is rapidly metabolized, and its metabolites are potent activators of glycolytic enzymes and lipogenic transcription factors, leading to a rapid accumulation of TAG in kidney (Hannou et al., 2018). The renal triacylglycerol accumulation was proven by most lipids in GL03 increasing in FB-intake group (Fig. 2F). Further, triacylglycerol would be converted to DAG, generating PC, LPC, and SM (Han, 2016), verified by the lipid alteration of GP01, SP02, and SP03 in FB-intake group (Fig. 2F). Moreover, excess free fructose (EFF) is defined as fructose-to-glucose ratios that exceed 1 (Dechristopher, 2015). FB contains more EFF, while FJ nearly does not. Although we have observed higher EFF contents in FB yield renal disorder, subsequent research is required to probe the molecular mechanism of high EFF-induced renal disorder.

On the contrary, FJ prevented metabolic syndrome with downregulated insulin resistance. Markers of insulin resistance, poor control of blood glucose levels, and systemic inflammation were associated with lower gut microbiome diversity (Zouiouich et al., 2021). Hence, the significantly higher alpha diversity in FJ-intake group would be conducive to downregulated insulin resistance. Moreover, the high F/B ratio association with obesity and metabolic syndrome seems to be a reasonably recurrent finding (Woting and Blaut, 2016), suggesting the lower F/B ratio prevents obesity and metabolic syndrome in FJ-intake group. Furthermore, the low F/B ratio mainly comes from the high abundance of bacterial taxa from Bacteroides, which are Bacterioidia (Class), Bacteroidales (Order), Muribaculaceae (Family), and Prevotella (Genus), and these above bacterial taxa are negatively correlated with metabolic syndrome. For instance, attenuated metabolic syndrome was related to the increased Bacteroidia (John et al., 2020). The enhanced Bacteroidales were positively correlated with the reduced metabolic syndrome of fat accumulation and lipid disorders (Xu et al., 2020). As a beneficial composition of gut microbiota, the increased richness of Muribaculaceae was an approach for metabolic syndrome alleviation (J. Chen et al., 2021; Z.-R. Li et al., 2021).

The flavonoids may be one of the reasons for the health benefit of FJ intake. Flavonoids, such as hesperidin and quercetin, could modulate

postprandial glycaemic response (Kerimi et al., 2019) and the gut microbiota structure to prevent metabolic diseases (Estruel-Amades et al., 2019; Porras et al., 2019), which might explain why 100% orange juice has a neutral effect on rats although naturally containing similar amounts of free sugars as sugar-sweetened beverage. Two key factors, the type of flavonoids and dose, are tightly related to the effect of flavonoids on gut microbiota structure. Flavonoids occur as aglycones, glycosides, and methylated derivatives (Kumar and Pandey, 2013). Among the 8 flavonoids, naringenin, quercetin, hesperetin, and nobiletin belong to aglycones, while narirutin, didymin, hesperidin, and vicenin 2 belong to glucosides, especially vicenin 2 containing 2 glycosides. Although vicenin 2 is 4.9 times higher in FJ compared to FB, it shows no significant correlation with the F/B ratio, while the other 7 flavonoids, especially naringenin and didymin belonging to flavonoid aglycones, with lower FC values of 3.3 and 3.1, are negatively correlated to the F/B ratio. Previous studies with inconsistent results have shown glucosides strongly affect the bioactivity of flavonoids: some studies showed that flavonoid glycosides enhanced more bioactivity than their flavonoid aglycones (Xiao, 2017), while others showed that glycosides showed no bioactivity (Steensma et al., 2006). Essentially, flavonoid glycosides are either hydrolyzed in the small intestine by specific enzymes or metabolized in the large intestine by the action of intestinal microbiota to yield aglycones to exert their biological function (Baky et al., 2022). Given our study, flavonoid aglycones exhibit more potent regulatory bioactivity for gut microbiota structure, which may be because the bioactivity of flavonoid aglycones is more direct, which reduces the uncertainty of the conversion of glycosides to aglycones. Furthermore, the different effects of flavonoid types and their thresholds on gut microbiota structure are worth exploring thoroughly. However, it is hard to identify all the differential bioactive metabolites due to the limited electronic database. Previous studies have revealed that pectin modulates the digestion and absorption of nutrients, regulates the composition and activity of the gut microbiota, and affects the production of short-chain fatty acids (J. Liu et al., 2020). Therefore, exploring the health effects of pectin in drinks, which is a comprehensive system, is very complex, and the contribution of pectin should never be ignored.

Disparate trends in the metabolic syndrome of rats were discovered in FJ-intake and FB-intake groups (Fig. 7). FJ improved alpha diversity and decreased F/B ratio of gut microbiota and prevented insulin resistance with the reduced food intake in FJ-intake group. However, FB possessed unchanged microbial diversity and F/B ratio, causing insulin resistance with renal triglyceride accumulation, increased kidney mass index as well as steadily improved weight change in FB-intake group.

5. Conclusions

In summary, the result here provided valid evidence that considering only the sugar content of 100% fruit juice is not a balanced approach, and the multi-bioactive metabolites (such as flavonoids) of FJ may positively impact host health compared with FB. The disparate health outcomes of foods with distinct processing degrees were further illuminated that FJ prevented insulin resistance while FB caused insulin resistance through the diet-microbiome-metabolic pathway axis. Our results clearly suggest that FJ with a lower processing degree, although naturally containing similar amounts of free sugars as FB, could be a healthier drink choice.

Institutional review board statement

The animal experiments were performed in the lab of the Institutional Animal Care and Use Committee of Beijing Vital River Laboratory Animal Technology Co., Ltd. All experimental procedures described here were conducted following the National Institutes of Health Guidelines on the Care and Use of Laboratory Animal of Institutional Animal Care and Use Committee of Beijing Vital River Laboratory Animal Technology Co., Ltd. The approve code is SCXK-2016–0006. The permission code is P2021032.
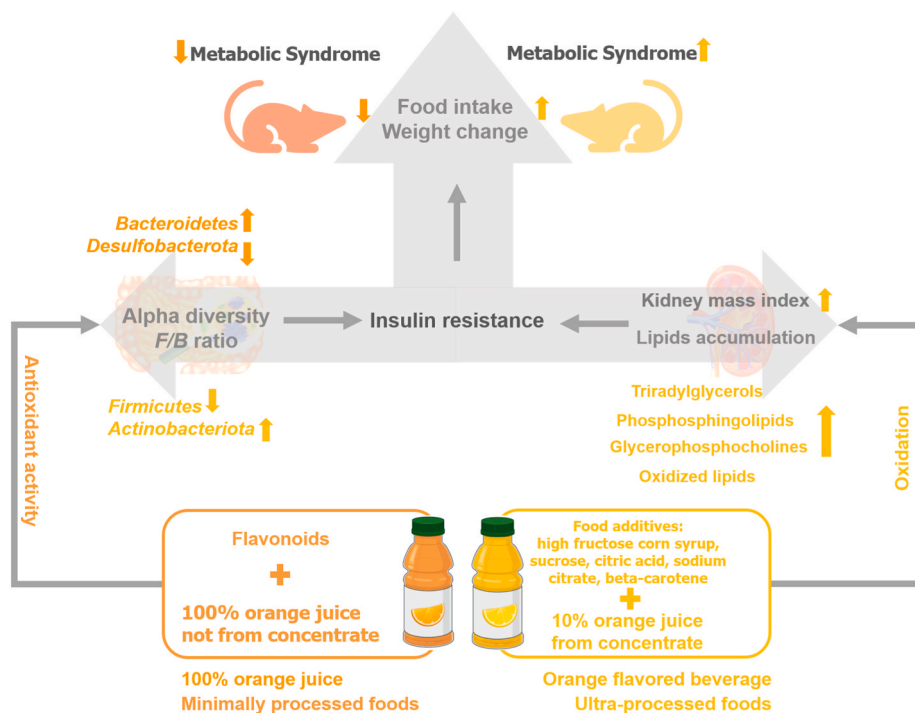

Fig. 7. The distinct health outcomes in SD rats are that FJ improved alpha diversity and decreased F/B ratio of gut microbiota, and prevented insulin resistance with the reduced food intake in FJ-intake group. In contrast, FB, which contains various food additives, possessed unchanged microbial diversity and F/B ratio, causing insulin resistance with renal triglyceride accumulation, increased kidney mass index and oxidation, and steadily improved weight change in FB-intake group.

CRediT authorship contribution statement

Kewen Wang: Formal analysis, Data curation, Writing – original draft. **Yang Zhao:** Writing – original draft. **Lei Xu:** Writing – original draft. **Xiaojun Liao:** Conceptualization, Supervision. **Zhenzhen Xu:** Conceptualization, Formal analysis, Methodology, Writing – review & editing, Supervision.

Declaration of competing interest

The authors declare that they have no known competing financial interests or personal relationships that could have appeared to influence the work reported in this paper.

Data availability

Data will be made available on request.

Acknowledgments

Appendix A. Supplementary data

Supplementary data to this article can be found online at https://doi.org/10.1016/j.crfs.2023.100454.

References

Anderson, G.H., 1995. Sugars, sweetness, and food intake. Am. J. Clin. Nutr. 62 (1 Suppl. l), 195S–202S.

Anderson, G.H., Woodend, D., 2003. Effect of glycemic carbohydrates on short-term satiety and food intake. Nutr. Rev. 61 (2), 17–26.

Asipu, A., Hayward, B.E., O'Reilly, J., Bonthron, D.T., 2003. Properties of normal and mutant recombinant human ketohexokinases and implications for the pathogenesis of essential fructosuria. Diabetes 52 (9), 2426–2432.

Baky, M.H., Elshahed, M., Wessjohann, L., Farag, M.A., 2022. Interactions between dietary flavonoids and the gut microbiome: a comprehensive review. Br. J. Nutr. 128 (4), 577–591.

Bulik, S., Holzhütter, H.G., Berndt, N., 2016. The relative importance of kinetic mechanisms and variable enzyme abundances for the regulation of hepatic glucose metabolism - insights from mathematical modeling. BMC Biol. 14 (1).

Caricilli, A.M., Saad, M.J.A., 2013. The role of gut microbiota on insulin resistance. Nutrients 5 (3), 829–851.

Chen, Z., Liang, Q., Wu, Y., Gao, Z., Kobayashi, S., Patel, J., Li, C., Cai, F., Zhang, Y., Liang, C., Chiba, H., Hui, S.P., 2020. Comprehensive lipidomic profiling in serum and multiple tissues from a mouse model of diabetes. Metabolomics 16 (11), 115.

Chen, J., Ding, X., Wu, R., Tong, B., Zhao, L., Lv, H., Meng, X., Liu, Y., Ren, B., Li, J., Jian, T., Li, W., 2021. Novel sesquiterpene glycoside from loquat leaf alleviates type 2 diabetes mellitus combined with nonalcoholic fatty liver disease by improving insulin resistance, oxidative stress, inflammation, and gut microbiota composition. J. Agric. Food Chem. 69 (47), 14176–14191.

Craig, E.A., Yan, Z., Zhao, Q.J., 2015. The relationship between chemical-induced kidney weight increases and kidney histopathology in rats. J. Appl. Toxicol. 35 (7), 729–736.

D'Elia, L., Dinu, M., Sofi, F., Volpe, M., Strazzullo, P., 2021. 100% Fruit juice intake and cardiovascular risk: a systematic review and meta-analysis of prospective and randomised controlled studies. Eur. J. Nutr. 60 (5), 2449–2467.

De Cosmo, S., Menzaghi, C., Prudente, S., Trischitta, V., 2013. Role of insulin resistance in kidney dysfunction: insights into the mechanism and epidemiological evidence. Nephrol DiaL Transpl 28 (1), 29–36.

De Gennaro Colonna, V., Bianchi, M., Pascale, V., Ferrario, P., Morelli, F., Pascale, W., Tomasoni, L., Turiel, M., 2009. Asymmetric dimethylarginine (ADMA): an endogenous inhibitor of nitric oxide synthase and a novel cardiovascular risk molecule. Med. Sci. Mon. Int. Med. J. Exp. Clin. Res.: Int. Med. J. Exper. Clin. Res. 15 (4), Ra91–101.

Dechristopher, L.R., 2015. Excess free fructose and childhood asthma. Eur. J. Clin. Nutr. 69 (12), 1371.

Estruel-Amades, S., Massot-Cladera, M., Pérez-Cano, F.J., Franch, À., Castell, M., Camps-Bossacoma, M., 2019. Hesperidin effects on gut microbiota and gut-associated lymphoid tissue in healthy rats. Nutrients 11 (2), 324.

Etxeberria, U., Arias, N., Boqué, N., Macarulla, M.T., Portillo, M.P., Martínez, J.A., Milagro, F.I., 2015. Reshaping faecal gut microbiota composition by the intake of trans-resveratrol and quercetin in high-fat sucrose diet-fed rats. Int. J. Paediatr. Dent. 26 (6), 651–660.

Food and Agriculture Organization of the United Nations, 2015. Guidelines on the Collection of Information on Food Processing through Food Consumption Surveys [R/OL]. https://www.fao.org/3/i4690e/i4690e.pdf.

Freije, S.L., Senter, C.C., Avery, A.D., Hawes, S.E., Jones-Smith, J.C., 2021. Association between consumption of sugar-sweetened beverages and 100% fruit juice with poor mental health among US adults in 11 US states and the District of Columbia. Prev. Chronic Dis. 18, E51.

General standard for fruit juices and nectars (CODEX STAN 247-2005), 2005. Codex Alimentarius Commission.

Guebre-Egziabher, F., Alix, P.M., Koppe, L., Pelletier, C.C., Kalbacher, E., Fouque, D., Soulage, C.O., 2013. Ectopic lipid accumulation: a potential cause for metabolic disturbances and a contributor to the alteration of kidney function. Biochimie 95 (11), 1971–1979.

Guido, J.A., Martinez Mier, E.A., S, A., 2011. Caries prevalence and its association with brushing habits, water availability, and the intake of sugared beverages. Int. J. Paediatr. Dent. 21 (6), 432–440.

Hagele, F.A., Busing, F., Nas, A., Aschoff, J., Gnadinger, L., Schweiggert, R., Carle, R., Bosy-Westphal, A., 2018. High orange juice consumption with or in-between three meals a day differently affects energy balance in healthy subjects. Nutr. Diabetes 8 (1), 19.

Han, X., 2016. Lipidomics for studying metabolism. Nat. Rev. Endocrinol. 12 (11), 668–679.

Hannou, S.A., Haslam, D.E., McKeown, N.M., Herman, M.A., 2018. Fructose metabolism and metabolic disease. J. Clin. Invest. 128 (2), 545–555.

Harvey, A.G., Catherine Nicole, L.A., Woodend, D.M., Wolever Thomas, M.S., 2002a. Inverse association between the effect of carbohydrates on blood glucose and subsequent short-term food intake in young men. Am. J. Clin. Nutr. (5), 1023–1030.

Harvey, G., Anderson, Nicole, L.A., Catherine, Dianne, M., Woodend, Thomas, M.S., Wolever, 2002b. Inverse association between the effect of carbohydrates on blood glucose and subsequent short-term food intake in young men. Am. J. Clin. Nutr. 76, 547–552.

He, F.-F., Li, Y.-M., 2020. Role of gut microbiota in the development of insulin resistance and the mechanism underlying polycystic ovary syndrome: a review. J. Ovarian Res. 13 (1), 73-73.

Hong, E., Lim, Y., Lee, E., Oh, M., Kwon, D., 2012. Tissue-specific and age-dependent expression of protein arginine methyltransferases (PRMTs) in male rat tissues. Biogerontology 13 (3), 329–336.

Jayalath, V.H., Souza, R.J.D., V, H., 2015. Sugar-sweetened beverage consumption and incident hypertension: a systematic review and meta-analysis of prospective cohorts. Am. J. Clin. Nutr. 102 (4), 914–921.

John, O.D., Mouatt, P., Majzoub, M.E., Thomas, T., Panchal, S.K., Brown, L., 2020. Physiological and metabolic effects of yellow mangosteen (Garcinia dulcis) rind in rats with diet-induced metabolic syndrome. Int. J. Mol. Sci. 21 (1), 272.

Johnson, A.E., Sidwick, K.L., Pirgozliev, V.R., Edge, A., Thompson, D.F., 2018. Metabonomic profiling of chicken eggs during storage using high-performance liquid chromatography-quadrupole time-of-flight mass spectrometry. Anal. Chem. 90 (12), 7489–7494.

Kerimi, A., Gauer, J.S., Crabbe, S., Cheah, J.W., Lau, J., Walsh, R., Cancalon, P.F., Williamson, G., 2019. Effect of the flavonoid hesperidin on glucose and fructose transport, sucrase activity and glycaemic response to orange juice in a crossover trial on healthy volunteers. Br. J. Nutr. 121 (7), 782–792.

Kotlyarov, S., Bulgakov, A., 2021. Lipid metabolism disorders in the comorbid course of nonalcoholic fatty liver disease and chronic obstructive pulmonary disease. Cells 10 (11), 2978.

Kumar, S., Pandey, A.K., 2013. Chemistry and Biological Activities of Flavonoids: an Overview. ScientificWorldJournal, 162750, 2013.

Lachowicz, S., Oszmianski, J., 2018. The influence of addition of cranberrybush juice to pear juice on chemical composition and antioxidant properties. J. Food Sci. Technol. 55 (9), 3399–3407.

Laparra, J.M., Sanz, Y., 2010. Interactions of gut microbiota with functional food components and nutraceuticals. Pharmacol. Res. 61 (3), 219–225.

Lartey, A., Meerman, J., Wijesinha-Bettoni, R., 2018. Why Food System Transformation Is Essential and How Nutrition Scientists Can Contribute. Ann Nutr Metab, pp. 193–201.

Li, Y., Wang, D.D., Satija, A., Ivey, K.L., Li, J., Wilkinson, J.E., Li, R., Baden, M., Chan, A. T., Huttenhower, C., Rimm, E.B., Hu, F.B., Sun, Q., 2021a. Plant-based diet index and metabolic risk in men: exploring the role of the gut microbiome. J. Nutr. 151 (9), 2780–2789.

Li, Z.-R., Jia, R.-B., Wu, J., Lin, L., Ou, Z.-R., Liao, B., Zhang, L., Zhang, X., Song, G., Zhao, M., 2021b. Sargassum fusiforme polysaccharide partly replaces acarbose against type 2 diabetes in rats. Int. J. Biol. Macromol. 170, 447–458.

Lima, A.C.D., Cecatti, C., Fidélix, M.P., Adorno, M.A.T., Sakamoto, I.K., Cesar, T.B., Sivieri, K., 2019. Effect of daily consumption of orange juice on the levels of blood glucose, lipids, and gut microbiota metabolites: controlled clinical trials. J. Med. Food 22 (2), 202–210.

Lin, L., Huang, Z., Gao, Y., Yan, X., Xing, J., Hang, W., 2011. LC-MS based serum metabonomic analysis for renal cell carcinoma diagnosis, staging, and biomarker discovery. J. Proteome Res. 10 (3), 1396–1405.

Lin, L., Huang, Z., Gao, Y., Chen, Y., Hang, W., Xing, J., Yan, X., 2012. LC-MS-based serum metabolic profiling for genitourinary cancer classification and cancer type-specific biomarker discovery. Proteomics 12 (14), 2238–2246.

Liu, H., Li, W., He, Q., Xue, J., Wang, J., Xiong, C., Pu, X., Nie, Z., 2017. Mass spectrometry imaging of kidney tissue sections of rat subjected to unilateral ureteral obstruction. Sci. Rep. 7, 41954.

Liu, J., Bi, J., McClements, D.J., Liu, X., Yi, J., Lyu, J., Zhou, M., Verkerk, R., Dekker, M., Wu, X., Liu, D., 2020. Impacts of thermal and non-thermal processing on structure and functionality of pectin in fruit- and vegetable- based products: a review. Carbohydr. Polym. 250, 116890.

Lustig, R.H., Schmidt, L.A., Brindis, C.D., 2012. The toxic truth about sugar. Nature 482 (7383), 27–29.

Malik, V.S., Popkin, B.M., Bray, G.A., Despres, J.P., Hu, F.B., 2010. Sugar-sweetened beverages, obesity, type 2 diabetes mellitus, and cardiovascular disease risk. Circulation 121 (11), 1356–1364.

Markopoulou, P., Papanikolaou, E., Analytis, A., Zoumakis, E., Siahanidou, T., 2019. Preterm birth as a risk factor for metabolic syndrome and cardiovascular disease in adult life: a systematic review and meta-analysis. J. Pediatr. 210, 69–80.e65.

Mikhail, N., 2009. The metabolic syndrome: insulin resistance. Curr. Hypertens. Rep. 11 (2), 156–158.

Monteiro, C., Cannon, G., Moubarac, J.-C., Levy, R., Louzada, M.L., Jaime, P., 2017. The UN Decade of Nutrition, the NOVA food classification and the trouble with ultra-processing. Publ. Health Nutr. 21 (1), 5–17.

Nair, A.B., Jacob, S., 2016. A simple practice guide for dose conversion between animals and human. J. Basic Clin. Pharm. 7 (2), 27–31.

Narain, A., Kwok, C.S., Mamas, M.A., 2016. Soft drinks and sweetened beverages and the risk of cardiovascular disease and mortality: a systematic review and meta-analysis. Int. J. Clin. Pract. 70 (10), 791–805.

Neergaard, J.S., Dragsbæk, K., Christiansen, C., Nielsen, H.B., Brix, S., Karsdal, M.A., Henriksen, K., 2017. Metabolic syndrome, insulin resistance, and cognitive dysfunction: does your metabolic profile affect your brain? Diabetes 66 (7), 1957–1963.

Neves, M.F., Trombin, V.G., Marques, V.N., Martinez, L.F., 2020. Global orange juice market: a 16-year summary and opportunities for creating value. Trop. Plant Pathol. 45 (3), 166–174.

Ng, N., Minh, H.V., Juvekar, S., Razzaque, A., Bich, T.H., Kanungsukkasem, U., Ashraf, A., Ahmed, S.M., Soonthornthada, K., 2009. Using the INDEPTH HDSS to build capacity for chronic non-communicable disease risk factor surveillance in low and middle-income countries. Glob. Health Action 2 (1), 7–18.

Porras, D., Nistal, E., Martínez-Flórez, S., Olcoz, J.L., Jover, R., Jorquera, F., González-Gallego, J., García-Mediavilla, M.V., Sánchez-Campos, S., 2019. Functional interactions between gut microbiota transplantation, quercetin, and high-fat diet determine non-alcoholic fatty liver disease development in germ-free mice. Mol. Nutr. Food Res. 63 (8), e1800930.

Posma, J.M., Garcia-Perez, I., Frost, G., Aljuraiban, G.S., Chan, Q., Van Horn, L., Daviglus, M., Stamler, J., Holmes, E., Elliott, P., Nicholson, J.K., 2020. Nutriome-metabolome relationships provide insights into dietary intake and metabolism. Nat. Food 1 (7), 426–436.

Remely, M., Haslberger, A.G., 2017. The microbial epigenome in metabolic syndrome. Mol. Aspect. Med. 54, 71–77.

Rezek, M., 1976. The role of insulin in the glucostatic control of food intake. Can. J. Physiol. Pharmacol. 54 (5), 650–665.

Rogers, P.J., Carlyle, J.A., Hill, A.J., Blundell, J.E., 1988. Uncoupling sweet taste and calories: comparison of the effects of glucose and three intense sweeteners on hunger and food intake. Physiol. Behav. 43 (5), 547–552.

Shefferly, A., Scharf, R.J., DeBoer, M.D., 2016. Longitudinal evaluation of 100% fruit juice consumption on BMI status in 2-5-year-old children. Pediatr. Obes. 11 (3), 221–227.

Sibal, L., Agarwal, S.C., Home, P.D., Boger, R.H., 2010. The role of asymmetric dimethylarginine (ADMA) in endothelial dysfunction and cardiovascular disease. Curr. Cardiol. Rev. 6 (2), 82–90.

Siervo, M., Corander, M., Stranges, S., Bluck, L., 2011. Post-challenge hyperglycaemia, nitric oxide production and endothelial dysfunction: the putative role of asymmetric dimethylarginine (ADMA). Nutrition, metabolism, and cardiovascular diseases. Nutr. Metabol. Cardiovasc. Dis. 21 (1), 1–10.

Steensma, A., Faassen-Peters, M.A., Noteborn, H.P., Rietjens, I.M., 2006. Bioavailability of genistein and its glycoside genistin as measured in the portal vein of freely moving unanesthetized rats. J. Agric. Food Chem. 54 (21), 8006–8012.

Su, H., Wan, C., Lei, C.-T., Zhang, C.-Y., Ye, C., Tang, H., Qiu, Y., Zhang, C., 2017. Lipid deposition in kidney diseases: interplay among redox, lipid mediators, and renal impairment. Antioxidants Redox Signal. 28 (10), 1027–1043.

Sydow, K., Mondon, C.E., Cooke, J.P., 2005. Insulin resistance: potential role of the endogenous nitric oxide synthase inhibitor ADMA. Vasc. Med. 10 (Suppl. 1), S35–S43.

Theodoridis, G.A., Gika, H.G., Want, E.J., Wilson, I.D., 2012. Liquid chromatography–mass spectrometry based global metabolite profiling: a review. Anal. Chim. Acta 711 (none), 7–16.

Tian, Y., Zhang, L., Wang, Y., Tang, H., 2012. Age-related topographical metabolic signatures for the rat gastrointestinal contents. J. Proteome Res. 11 (2), 1397–1411.

Tiedemann, L.J., Schmid, S.M., Hettel, J., Giesen, K., Francke, P., Büchel, C., Brassen, S., 2017. Central insulin modulates food valuation via mesolimbic pathways. Nat. Commun. 8, 16052.

Tu, J., Yin, Y., Xu, M., Wang, R., Zhu, Z.J., 2017. Absolute quantitative lipidomics reveals lipidome-wide alterations in aging brain. Metabolomics 14 (1), 5.

Unger, R.H., Scherer, P.E., 2010. Gluttony, sloth and the metabolic syndrome: a roadmap to lipotoxicity. Trends Endocrinol. Metabol. 21 (6), 345–352.

Vandevijvere, S., Barquera, S., Caceres, G., Corvalan, C., Karupaiah, T., Kroker-Lobos, M. F., L'Abbé, M., Ng, S.H., Phulkerd, S., Ramirez-Zea, M., 2019. An 11-country study to benchmark the implementation of recommended nutrition policies by national governments using the Healthy Food Environment Policy Index, 2015-2018. Obes. Rev. 20, 57–66.

Vega, G.L., 2004. Obesity and the metabolic syndrome. Minerva Endocrinol. 29 (2), 47–54.

Wang, K., Xu, Z., 2022. Comparison of freshly squeezed, Non-thermally and thermally processed orange juice based on traditional quality characters, untargeted metabolomics, and volatile overview. Food Chem. 373, 131430.

Wang, B., Wang, X., Bei, J., Xu, L., Zhang, X., Xu, Z., 2021a. Development and validation of an analytical method for the quantification of arabinose, galactose, glucose, sucrose, fructose, and maltose in fruits, vegetables, and their products. Food Anal. Methods 4, 1–12.

Wang, K., Xu, L., Wang, X., Chen, A., Xu, Z., 2021b. Discrimination of beef from different origins based on lipidomics: a comparison study of DART-QTOF and LC-ESI-QTOF. LWT 149, 111838.

Wang, K., Wang, X., Zhang, L., Chen, A., Yang, S., Xu, Z., 2022. Identification of novel biomarkers in chilled and frozen chicken using metabolomics profiling and its application. Food Chem. 393, 133334.

Willis, H.J., Slavin, J.L., 2020. The influence of diet interventions using whole, plant food on the gut microbiome: a narrative review. J. Acad. Nutr. Diet. 120 (4), 608–623.

Woting, A., Blaut, M., 2016. The intestinal microbiota in metabolic disease. Nutrients 8 (4).

Xiao, J., 2017. Dietary flavonoid aglycones and their glycosides: which show better biological significance? Crit. Rev. Food Sci. Nutr. 57 (9), 1874–1905.

Xie, G., Zhong, W., Zheng, X., Li, Q., Qiu, Y., Li, H., Chen, H., Zhou, Z., Jia, W., 2013. Chronic ethanol consumption alters mammalian gastrointestinal content metabolites. J. Proteome Res. 12 (7), 3297–3306.

Xu, Y., Ai, C., Jiang, P., Sun, X., Liu, Y., Jiang, G., Song, S., 2020. Oligosaccharides from Gracilaria lemaneiformis better attenuated high fat diet-induced metabolic syndrome by promoting the Bacteroidales proliferation. Food Funct. 11 (1), 1049–1062.

Zheng, M., Allman-Farinelli, M., Heitmann, B.L., Rangan, A., 2015. Substitution of sugar-sweetened beverages with other beverage alternatives: a review of long-term health outcomes. J. Acad. Nutr. Diet. 115 (5), 767–779.

Zouiouich, S., Loftfield, E., Huybrechts, I., Viallon, V., Louca, P., Vogtmann, E., Wells, P. M., Steves, C.J., Herzig, K.-H., Menni, C., Jarvelin, M.-R., Sinha, R., Gunter, M.J., 2021. Markers of metabolic health and gut microbiome diversity: findings from two population-based cohort studies. Diabetologia 64 (8), 1749–1759.